

# Quantum receivers with squeezing and photon-number-resolving detectors for $M$ -ary coherent state discrimination

Shuro Izumi,<sup>1,2</sup> Masahiro Takeoka,<sup>1,3</sup> Kazuhiro Ema,<sup>2</sup> and Masahide Sasaki<sup>1</sup>

<sup>1</sup> National Institute of Information and Communications Technology, 4-2-1 Nukui-kita, Koganei, Tokyo 184-8795, Japan

<sup>2</sup> Sophia University, 7-1 Kioicho, Chiyoda-ku, Tokyo 102-8554, Japan

<sup>3</sup> Raytheon BBN Technologies, 10 Moulton Street, Cambridge, MA 02138, USA

(Dated: September 12, 2018)

We propose quantum receivers with optical squeezing and photon-number-resolving detector (PNRD) for the near-optimal discrimination of quaternary phase-shift-keyed coherent state signals. The basic scheme is similar to the previous proposals (e.g. Phys. Rev. A **86**, 042328 (2012)) in which displacement operations, on-off detectors, and electrical feedforward operations were used. Here we study two types of receivers where one installs optical squeezings and the other uses PNRDs instead of on-off detectors. We show that both receivers can attain lower error rates than that by the previous scheme. In particular, we show the PNRD based receiver has a significant gain when the ratio between the mean photon number of the signal and the number of the feedforward steps is relatively high, in other words, the probability of detecting two or more photons at each detector is not negligible. Moreover, we show that the PNRD based receiver can suppress the errors due to dark counts, which is not possible by the on-off detector based receiver with a small number of feedforwards.

PACS numbers: 03.67.Hk, 03.67.-a

## I. INTRODUCTION

Coherent states are known as the best signal carriers in optical communication owing to their loss-tolerant property. Coherent states propagating through a lossy channel remain in a pure coherent state with decreased amplitude while more exotic states such as photon number states easily lose their purity in a lossy channel. In fact, the ultimate channel capacity in a lossy bosonic channel can be attained by using coherent state carriers, appropriate classical encoding and a quantum mechanically optimal decoding (measurement) over a sequence of coherent states [1].

Implementation of such kind of quantum collective decoding is still challenging. Currently, attentions are paid to implementing quantum receivers for detecting each coherent pulse separately at a smaller error rate than the conventional limit (*standard quantum limit* : SQL) which is attained by homodyne/heterodyne receivers.

The quantum mechanical bound of the minimum error rate is called the Helstrom bound and is known to be significantly lower than the SQL. Physical implementations of the optimal quantum receiver to achieve the Helstrom bound were studied theoretically in the 1970's by Kennedy and Dolinar [2–4] and recently further investigated from a more practical point of view [5–10]. Experimentally the super-SQL performances even without compensating for imperfections were demonstrated for both on-off-keying (OOK) [11, 12] and binary phase-shift-keying (BPSK) [13, 14].

More recently, attention has also been paid to the  $M$ -ary signal with  $M > 2$  where one can encode the message in pulses more densely [15–21]. Bondurant [15] extended Dolinar's optimal binary signal discrimination scheme and proposed near-optimal receivers for quater-

nary phase-shift-keying (QPSK), which consists of a local oscillator, an on-off detector (which distinguish only zero or non-zero photons), and an infinitely fast feedback operation. Later, more practical schemes assuming the finite number of feedforward steps have been studied [16, 17] and very recently the super-SQL performance was experimentally demonstrated [18]. As another approach, the QPSK discrimination by a hybrid receiver of homodyne and on-off detections was also proposed [19]. In addition, the near-optimal discrimination was also demonstrated for the pulse-position coding [22, 23]. In all of these schemes, the near-optimal performance is achieved by inducing effective optical nonlinearities via an on-off detection and the ultrafast electrical feedback (or feedforward) operation.

In this paper, we theoretically show that additional optical nonlinear processes, squeezing and photon-number-resolving detector (PNRD), are also useful for the QPSK coherent state discrimination. For the binary case, it was shown that the squeezing can slightly improve the error rate performance [9]. We show that the similar effect can be observed by installing squeezers into the QPSK receiver scheme we proposed previously [17].

PNRD is also known as an attractive device to induce an effective optical nonlinearity in optical quantum information processing [24]. For the coherent state discrimination task, PNRD has been applied to implement a generalized (non-projective) measurement of discriminating binary states with an inconclusive result [25, 26]. Furthermore, a benefit of employing PNRD for  $M$ -ary coherent state discrimination was also implied in [16]. Here we apply PNRD into the QPSK receiver based on [17] and show that it can achieve the near-optimal error performance even if the number of feedback steps is relatively small. In other words, PNRDs can decrease the

number of feedforward steps to attain the same performance. In addition, we show that this scheme is highly robust against the dark counts.

In Sec. II, we propose and analyze the QPSK receiver with the squeezing operation. The receiver with PNRD is proposed and numerically simulated in Sec. III. Section IV concludes the paper.

## II. DISPLACEMENT RECEIVER WITH SQUEEZING OPERATION

In this section, we apply the squeezing operations into the displacement receiver proposed in [17]. The signals to be discriminated are  $M$ -PSK coherent states defined as

$$|\alpha_m\rangle = |\alpha u^m\rangle, \quad u = e^{2\pi i/M}, \quad (1)$$

where  $m = 0, 1, \dots, M-1$  and  $\alpha$  is chosen to be real without loss of generality. Throughout this paper, we fix  $M = 4$  and assume equal *a priori* probabilities, i.e.  $p_m = 1/M$  for all  $m$ .

A schematic of the receiver is depicted in Fig. 1. It consists of beam splitters, displacement operations, squeezing, and on-off detectors. The QPSK signal is split into three ports via two beam splitters having reflectance  $R_1$  and  $R_2$ , respectively. At each port, the displacement operation is applied. The operator is given by  $\hat{D}(\gamma) = \exp[(\gamma\hat{a}^\dagger - \gamma^*\hat{a})]$  which shifts the amplitude of coherent state as  $\hat{D}(\gamma)|\beta\rangle = |\beta + \gamma\rangle$ . It is widely known that  $\hat{D}(\gamma)$  is realized by a beam splitter with transmittance  $\tau \approx 1$  and relatively strong local oscillator  $|\gamma/\sqrt{\tau}\rangle$ . In our scheme it is applied such that one of the four symbols is displaced to be close to the vacuum state (signal nulling). The previous works [9, 12–14, 17, 19, 22, 23] showed that the optimal displacement minimizing the average error is slightly different from the exact nulling, which is taken into account in here as well. The target signals to be nulled at port A, B, and C are  $m = 0, 2, 1$ .

The displaced signal at each port is then squeezed by the squeezing operation  $\hat{S}(\xi) = \exp[(\xi^*\hat{a}^2 - \xi\hat{a}^{\dagger 2})/2]$ , where  $\xi = re^{i\phi}$  is the complex squeezing parameter, and then detected by an on-off detector which distinguish if the signal is the nulled one or not. The on-off detection process at three ports are described by an appropriate set of three-mode measurement operators  $\{\hat{\Pi}_i\}$  ( $i = 0, 1, 2, 3$ ) and the correct detection probabilities are then given by

$$P(i|i) = \langle \Psi_i | \hat{\Pi}_i | \Psi_i \rangle. \quad (2)$$

From them, we obtain the average error probability as

$$P_e = 1 - \frac{1}{4} \sum_{i=0}^3 P(i|i). \quad (3)$$

The parameters of the beam splitters, the displacements, and the squeezings are numerically optimized to minimize  $P_e$ . Details of the derivation of Eq. (3) and the optimized parameters are described in Appendix A.

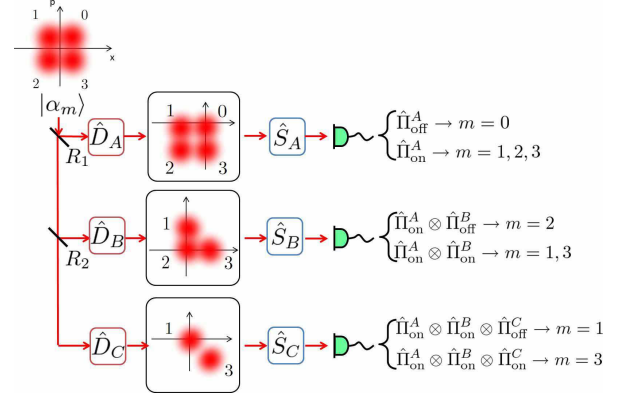


FIG. 1: (Color online) Displacement receiver with three-port detection structure without feedforward operations. The squeezing operations are applied to the displaced signals.

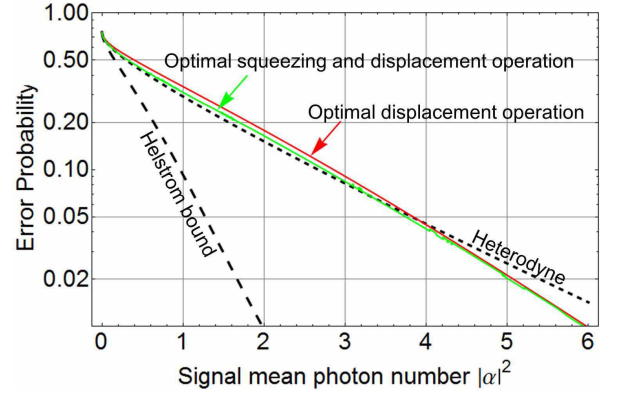


FIG. 2: (Color online) Average error rates for QPSK signal discrimination without applying the feedforward. The optimized displacements and squeezings receiver (green line) and the optimized displacements receiver (red line).  $\eta = 1$  and  $\nu = 0$ . Throughout this paper, the Helstrom bound and the heterodyne limit are represented by the black dashed and dotted line respectively.

In Fig. 2, we plot the average error rate of the proposed receiver which is compared with that of the receiver without squeezing [17], heterodyne receiver, and the Helstrom bound.

We observe an improvement of the performance by introducing squeezing operations in the small photon number region  $|\alpha|^2 \leq 4$ . However, the improvement is extremely small and thus it is expected that the gain would disappear when the system imperfections are taken into account. To observe a significant gain in this approach, one may need higher order nonlinear optical processes.

### III. DISPLACEMENT RECEIVER WITH PHOTON NUMBER RESOLVING DETECTORS

According to Ref. [17] the error rate for QPSK can be drastically improved by employing and repeating the feedforward that is based on the binary information from the on-off detector, which allows us to set the value of the displacement at the  $j$ th branch  $\hat{D}_j(\cdot)$  depending on the outcome from the  $(j-1)$ th branch. Additionally, the error rate performance of the feedforward receiver can be further increased by refining the feedforward rule by adopting the maximization of *a posteriori* probabilities. However, the *a posteriori* probabilities can be more precisely estimated by replacing the conventional on-off detectors with the PNRDs, because the amplitudes of signals are different from each other.

In this section, we study the displacement receiver allowing the use of PNRDs instead of on-off detectors and the feedforwards based on the Bayesian updating. The measurement operator of the PNRD for the  $n$ -photon detection is described by [28],

$$\hat{\Pi}_n = e^{-\nu} \sum_{l=0}^n \sum_{k=n-l}^{\infty} \frac{\nu^l}{l!} C_{n-l}^k \eta^{n-l} (1-\eta)^{k-(n-l)} |k\rangle \langle k|, \quad (4)$$

where  $C_{n-l}^k$  is the binomial coefficient. The probability of detecting  $n$  photons for the coherent state input  $|\beta\rangle$  is thus given by

$$P(n|\beta) = \langle \beta | \hat{\Pi}_n | \beta \rangle = e^{-\nu - \eta |\beta|^2} \frac{(\nu + \eta |\beta|^2)^n}{n!}. \quad (5)$$

The schematic of the receiver is shown in Fig. 3, which

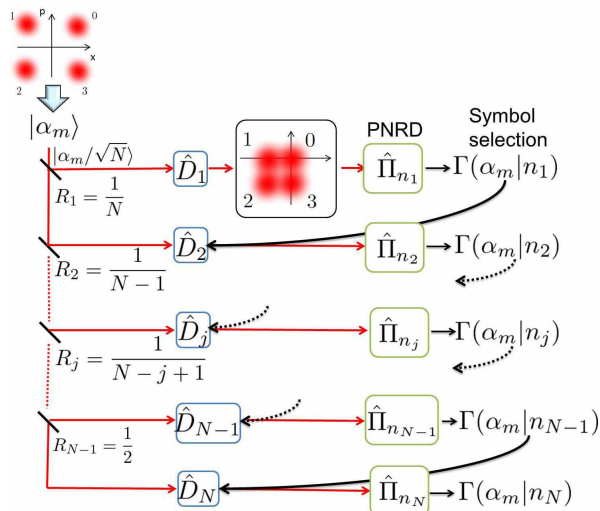


FIG. 3: (Color online) The displacement receiver consisting of  $N$ -step feedforward operations. The nulling symbol  $m_j$  on the  $j$ th stage is determined by the *a posteriori* probabilities on the  $(j-1)$ th stage.

is similar to those described in [16, 17] except that the on-off detectors are replaced by the PNRDs. The input signal is equally split into  $N$  ports via  $N-1$  beam splitters. We denote the nulling symbol on the  $j$ th stage as  $m_j$ . The nulling symbol at the first port is set to be  $m_1 = 0$  while the symbols  $m_j$  ( $j \geq 2$ ) are chosen to have the maximum *a posteriori* probability. The *a posteriori* probability for after detecting  $n_j$  photons at the  $j$ th stage is given by

$$\Gamma(\alpha_m | n_j) = \frac{\Gamma(\alpha_m | n_{j-1}) P(n_j | (\alpha_m - \alpha_{m_j}) / \sqrt{N})}{\sum_{l=0}^M \Gamma(\alpha_l | n_{j-1}) P(n_j | (\alpha_l - \alpha_{m_j}) / \sqrt{N})} = \frac{p_m \prod_{h=1}^j P(n_h | (\alpha_m - \alpha_{m_h}) / \sqrt{N})}{\sum_{l=0}^M p_l \prod_{h=1}^j P(n_h | (\alpha_l - \alpha_{m_h}) / \sqrt{N})}, \quad (6)$$

where  $p_m$  denotes the *a priori* probability.

We first derived an analytical expression of the average error rate assuming  $\nu = 0$ . In this case, once photons are detected from the signal in which  $m_j$  is nulled, we have  $\Gamma(\alpha_{m_j} | n_j) = 0$  and thus Eq. (6) is drastically simplified.

Fig. 4 shows the error rates of the  $N$ -step feedforward receivers ( $N = 3, 4, 5, 10$ ) with ideal PNRDs ( $\nu = 0$ ,  $\eta = 1$ , solid lines) and on-off detectors (dot-dashed lines). Remarkably low error rates are obtained for the PNRD based receiver in the region of small  $N$ . For larger  $N$ , the performance of the both receivers almost coincide since multi-use of on-off detectors at feedforward effectively resolves the number of photons in the original signal. The error rates for the PNRD receiver show step-like curves. At each feedforward step, with a given outcome  $n$ , we chose  $\alpha_m$  which maximizes  $\Gamma(\alpha_m | n)$  as the next nulling signal. In other words, the feedforward behavior highly depends on the classification  $\{n | \Gamma(\alpha_m | n) \geq \Gamma(\alpha_l | n) (l \neq m)\}$ . Due to the discrete nature of photon number, such a classification varies discretely as a function of  $|\alpha|^2$  resulting in the step-like curves on the averaged error performance.

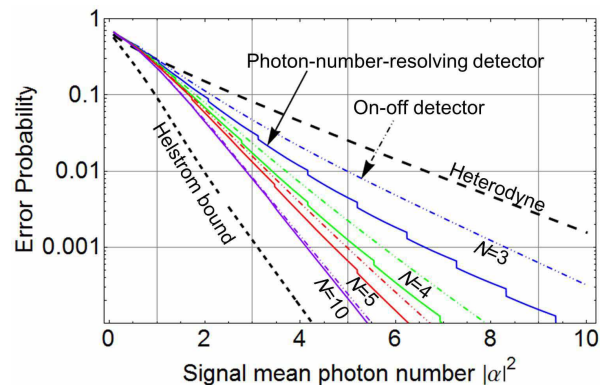


FIG. 4: (Color online) The displacement receiver consisting of  $N$ -step feedforward operations. Solid and dot-dashed lines denote the error probabilities for the PNRD detection and the on-off detection respectively.

For non-zero  $\nu$ , on the other hand, the analytical derivation of the error rate is almost intractable since all  $\Gamma(\alpha_{m_j}|n_j)$  could remain finite even after the  $j$ th stage. We therefore evaluate the error performance with non-ideal detectors by Monte Carlo simulations. Fig. 5(a) and (b) show the error rates for the on-off detectors and the PNRDs, respectively. We examined the performance for various  $\nu$  with  $\eta = 1$  and  $N = 3$ . For the on-off detectors (Fig. 5(a)), the error rates are saturated at  $P_e \approx \nu$ , which implies that the dark counts seriously limits the performance of the receiver. On the other hand, the PNRD based receiver is clearly free from the saturation problem (Fig. 5(b)). Since PNRD can discriminate incident photon numbers, it can exclude the events for dark counts from those for real signals to a certain extent, especially in the region where  $|\alpha|^2 \gg \nu$ . This reflects the robustness of the PNRD based receiver against the dark counts. Apparently, this is impossible by on-off detectors under condition having the same number of feedforward steps. Note that the robustness against the dark counts

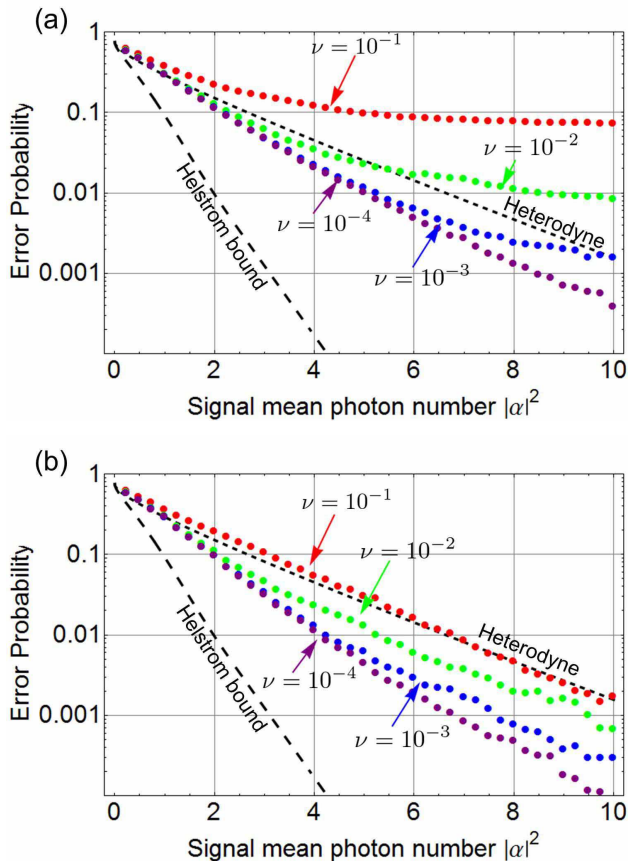


FIG. 5: (Color online) Degradation of the error rates depending on the dark count probability  $\nu$  for (a) on-off detector, and (b) PNRD. The feedforward steps and the detection efficiency are fixed at  $N = 3$  and  $\eta = 1$  in both figures. Each plot is given by a Monte Carlo simulation with  $10^5$  trials. Non-monotonic fluctuations of the plots at relatively high  $|\alpha|^2$  are due to the statistical errors of the simulation.

could be observed even with the on-off detectors if one allows large  $N$  since it effectively provides the number resolving ability as mentioned above.

We also evaluate the dependence on the detector efficiency  $\eta$  with  $\nu = 10^{-3}$  and  $N = 3$ . Fig. 6(a) shows that the detector efficiency 90% is at least required for the on-off detector to obtain the performance beyond the heterodyne limit, however, the requirement for the detector efficiency can be decreased to 70% by employing the PNRDs in place of the on-off detectors.

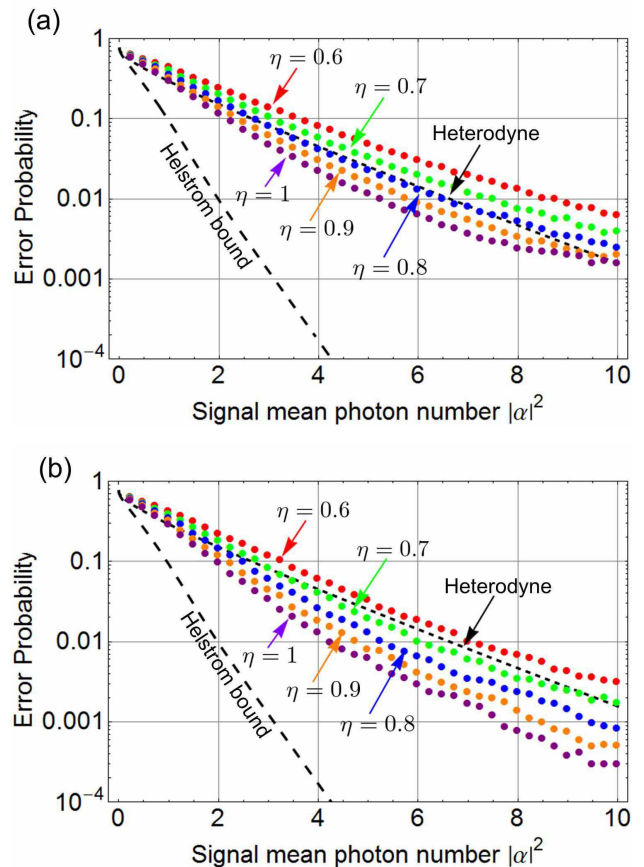


FIG. 6: (Color online) Degradation of the error probabilities depending on the detection efficiency  $\eta$  for (a) on-off detector, (b) PNRD. The feedforward steps and the dark count probability are fixed at  $N = 3$  and  $\nu = 10^{-3}$ .

#### IV. CONCLUSIONS

We proposed two quantum receivers for  $M$ -ary coherent state discrimination. The first one consists of displacements, on-off detectors, and squeezers without feedforward (or feedback) operations. The theoretical results showed that squeezing operation can slightly increase the performance at the weak signal region compared to the scheme without feedforward nor squeezing, presented in [17].

The second one consists of displacements, PNRDs, and feedforward operations. We numerically demonstrated that, for the fixed number of feedforward steps, the PNRD based receiver shows sufficiently better performance than the on-off detector based receivers [16–18]. In other words, PNRD can decrease the number of feedforward steps. It was also shown that the PNRD receiver is robust against the dark count which strictly limits the performance of photon counting based receivers in a relatively higher photon number regime. Though our analyses are concentrated on the QPSK signals, we emphasize that we can generalize these receivers to the  $M$ -ary signals ( $M > 4$ ) in a straightforward way.

Our results show that the PNRD receiver is a feasible scheme with the current technology and could achieve smaller error rates with a reduced number of feedforward steps. Fewer feedforward steps will allow us to detect the shorter pulsewidth or higher repetition rate signals, which are an important figure of merit toward implementing the practical application of quantum receivers.

Finally, from a theoretical point of view, an interesting future issue is to investigate how to fill the gap between the ideal performance of the feedforward based receiver and the exact Helstrom bound for the QPSK signals. It could be achieved by the additional nonlinear process e.g. replacing the beamsplitters with higher order nonlinear couplings.

## V. ACKNOWLEDGEMENT

This work was supported by the Founding Program for World-Leading Innovative R&D on Science and Technology (FIRST).

### Appendix A: Displacement receiver with squeezing operation: Formulation

In this appendix, we describe detailed derivations of  $|\Psi_i\rangle$  and  $\Pi_i$  discussed in Sec. II, which are necessary to calculate Eq. (2). As illustrated in Fig. 1, the signal is split into three ports and at each port, displaced and squeezed before the on-off detection. Thus the state just before the detection is generally in the squeezed coherent state  $|\xi; \beta\rangle$ . It is described in photon number bases as,

$$\begin{aligned} |\xi; \beta\rangle &= \hat{S}(\xi)\hat{D}(\beta)|0\rangle \\ &= e^{-\frac{|\beta|^2}{2} + \beta^2 \frac{\kappa^*}{2\mu}} \sum_{n=0}^{\infty} \frac{1}{\sqrt{n! \mu}} \left[ \frac{\kappa}{2\mu} \right]^{\frac{n}{2}} H_n\left(\frac{\beta}{\sqrt{2\mu\kappa}}\right) |n\rangle, \end{aligned} \quad (\text{A1})$$

where  $H_n$  is the  $n$ th Hermite polynomial,  $\mu = \cosh r$  and  $\kappa = e^{i\phi} \sinh r$  [27]. Let  $\beta_j$  and  $\xi_j$  be the displacement and squeezing parameters, respectively, at port  $j = A, B, C$ . After applying the displacements and squeezings,  $|\alpha_m\rangle$  is transformed to a three-mode state  $|\Psi_m\rangle$  where

$$\begin{aligned} |\Psi_0\rangle_{ABC} &= |\xi_A; \beta_A\rangle_A \\ &\otimes \left| \xi_B; \sqrt{(1-R_1)R_2}(\alpha_0 - \alpha_2) + \beta_B \right\rangle_B \\ &\otimes \left| \xi_C; \sqrt{(1-R_1)(1-R_2)}(\alpha_0 - \alpha_1) + \beta_C \right\rangle_C, \end{aligned} \quad (\text{A2})$$

$$\begin{aligned} |\Psi_1\rangle_{ABC} &= \left| \xi_A; \sqrt{R_1}(\alpha_1 - \alpha_0) + \beta_A \right\rangle_A \\ &\otimes \left| \xi_B; \sqrt{(1-R_1)R_2}(\alpha_1 - \alpha_2) + \beta_B \right\rangle_B \\ &\otimes |\xi_C; \beta_C\rangle_C, \end{aligned} \quad (\text{A3})$$

$$\begin{aligned} |\Psi_2\rangle_{ABC} &= \left| \xi_A; \sqrt{R_1}(\alpha_2 - \alpha_0) + \beta_A \right\rangle_A \otimes |\xi_B; \beta_B\rangle_B \\ &\otimes \left| \xi_C; \sqrt{(1-R_1)(1-R_2)}(\alpha_2 - \alpha_1) + \beta_C \right\rangle_C, \end{aligned} \quad (\text{A4})$$

$$\begin{aligned} |\Psi_3\rangle_{ABC} &= \left| \xi_A; \sqrt{R_1}(\alpha_3 - \alpha_0) + \beta_A \right\rangle_A \\ &\otimes \left| \xi_B; \sqrt{(1-R_1)R_2}(\alpha_3 - \alpha_2) + \beta_B \right\rangle_B \\ &\otimes \left| \xi_C; \sqrt{(1-R_1)(1-R_2)}(\alpha_3 - \alpha_1) + \beta_C \right\rangle_C. \end{aligned} \quad (\text{A5})$$

Note that the parameters optimized in Sec. II are  $R_1$ ,  $R_2$ ,  $\beta_A$ - $\beta_C$ , and  $\xi_A$ - $\xi_C$ .

An on-off detector only discriminates zero or non-zero photons. Its measurement operators are given by

$$\hat{\Pi}_{\text{off}} = e^{-\nu} \sum_{n=0}^{\infty} (1-\eta)^n |n\rangle \langle n|, \quad (\text{A6})$$

$$\hat{\Pi}_{\text{on}} = \hat{I} - \hat{\Pi}_{\text{off}}, \quad (\text{A7})$$

where  $\nu$  is the dark count probability and  $\eta$  is the detection efficiency. In our scheme three on-off detectors are used and the signal decision is carried out by the following combination of detection outcomes:

$$\begin{aligned} \hat{\Pi}_0 &= \hat{\Pi}_{\text{off}}^A \otimes \hat{I}^B \otimes \hat{I}^C, \\ \hat{\Pi}_1 &= \hat{\Pi}_{\text{on}}^A \otimes \hat{\Pi}_{\text{off}}^B \otimes \hat{I}^C, \\ \hat{\Pi}_2 &= \hat{\Pi}_{\text{on}}^A \otimes \hat{\Pi}_{\text{on}}^B \otimes \hat{\Pi}_{\text{off}}^C, \\ \hat{\Pi}_3 &= \hat{\Pi}_{\text{on}}^A \otimes \hat{\Pi}_{\text{on}}^B \otimes \hat{\Pi}_{\text{on}}^C, \end{aligned} \quad (\text{A8})$$

where  $\hat{I}$  is an identity operator. These descriptions allow us to calculate the probability  $\langle \Psi_i | \Pi_j | \Psi_i \rangle$ . In general, the probability of having an ‘‘off’’ outcome for the squeezed coherent state  $|\xi; \alpha_m\rangle$  is given by

$$\begin{aligned} P_{\text{off}} &= \langle \xi; \alpha_m | \hat{\Pi}_{\text{off}} | \xi; \alpha_m \rangle \\ &= e^{-\nu - \alpha^2 \{1 - \tanh r \cos(\frac{2m+1}{2}\pi - \phi)\}} \\ &\times \sum_{n=0}^{\infty} \frac{(1-\eta)^n}{n! \mu} \left[ \frac{|\kappa|}{2\mu} \right]^n \left| H_n\left(\frac{\alpha}{\sqrt{2\mu\kappa}}\right) \right|^2. \end{aligned} \quad (\text{A9})$$

- 
- [1] V. Giovannetti, S. Guha, S. Lloyd, L. Maccone, J. H. Shapiro, and H. P. Yuen, *Phys. Rev. Lett.* **92**, 027902 (2004).
- [2] C. W. Helstrom, *Quantum Detection and Estimation Theory* (Academic Press, New York, 1976).
- [3] R. S. Kennedy, Research Laboratory of Electronics, MIT, Quarterly Progress Report No. 108, 1973 (unpublished), p. 219.
- [4] S. Dolinar, Research Laboratory of Electronics, MIT, Quarterly Progress Report No. 111, 1973 (unpublished), p. 115.
- [5] M. Sasaki and O. Hirota, *Phys. Rev. A* **54**, 2728, (1996).
- [6] J. M. Geremia, *Phys. Rev. A* **70**, 062303, (2004).
- [7] M. Takeoka, M. Sasaki, P. van Loock, and N. Lütkenhaus, *Phys. Rev. A* **71**, 022318 (2005).
- [8] M. Takeoka, M. Sasaki, and N. Lütkenhaus, *Phys. Rev. Lett.* **97**, 040502 (2006).
- [9] M. Takeoka and M. Sasaki, *Phys. Rev. A* **78**, 022320 (2008).
- [10] A. Assalini, N. Dalla Pozza, and G. Pierobon, *Phys. Rev. A* **84**, 022342 (2011).
- [11] R. L. Cook, P. J. Martin, and J. M. Geremia, *Nature* **446**, 774 (2007).
- [12] K. Tsujino, D. Fukuda, G. Fujii, S. Inoue, M. Fujiwara, M. Takeoka, and M. Sasaki, *Opt. Express* **18**, 8107 (2010).
- [13] C. Wittmann, M. Takeoka, K. N. Cassemiro, M. Sasaki, G. Leuchs, and U. L. Andersen, *Phys. Rev. Lett.* **101**, 210501 (2008).
- [14] K. Tsujino, D. Fukuda, G. Fujii, S. Inoue, M. Fujiwara, M. Takeoka, and M. Sasaki, *Phys. Rev. Lett.* **106**, 250503 (2011).
- [15] R. S. Bondurant, *Opt. Lett.* **18**, 1896 (1993).
- [16] F. E. Becerra, J. Fan, G. Baumgartner, S. V. Polyakov, J. Goldhar, J. T. Kosloski, and A. Migdall, *Phys. Rev. A* **84**, 062324 (2011).
- [17] S. Izumi, M. Takeoka, M. Fujiwara, N. Dalla Pozza, A. Assalini, K. Ema, and M. Sasaki, *Phys. Rev. A* **86**, 042328 (2012).
- [18] F. E. Becerra, J. Fan, G. Baumgartner, J. Goldhar, J. T. Kosloski, and A. Migdall, *Nature Photon.* **7**, 147 (2013).
- [19] C. R. Müller, M. A. Usuga, C. Wittmann, M. Takeoka, C. Marquardt, U. L. Andersen, and G. Leuchs, *New J. Phys.* **14**, 083009 (2012).
- [20] M. Osaki, M. Ban, and O. Hirota, *Phys. Rev. A* **54**, 1691 (1996).
- [21] R. Nair and B. J. Yen, S. Guha, J. H. Shapiro, and S. Pirandola, *Phys. Rev. A* **86**, 022306 (2012).
- [22] S. Guha, J. L. Habif, and M. Takeoka, *J. Mod. Opt.* **58**, 257 (2011).
- [23] J. Chen, J. L. Habif, Z. Dutton, R. Lazarus, and S. Guha, *Nature Photon.* **6**, 374 (2012).
- [24] S. D. Bartlett and B. C. Sanders, *Phys. Rev. A* **65**, 042304 (2002).
- [25] C. Wittmann, U. L. Andersen, M. Takeoka, D. Sych and G. Leuchs, *Phys. Rev. Lett.* **104**, 100505 (2010).
- [26] C. Wittmann, U. L. Andersen, M. Takeoka, D. Sych and G. Leuchs, *Phys. Rev. A* **81**, 062338 (2010).
- [27] L. Mandel and E. Wolf, *Optical Coherence and Quantum Optics* (Cambridge U. Press, Cambridge, 1995).
- [28] S. M. Barnett, L. S. Phillips, D. T. Pegg, *Opt. Commun.* **158**, 45 (1998).